Original Article

Synergistic effects of the combination of Endostar and radiotherapy against hepatocellular carcinoma in a mouse model

Jundong Feng^{1,2}, Wei Luo³, Shukui Qin^{2,4}, Qiong Wu⁵, Xiaoping Wang⁴, Xiaojin Yin³, Xinchen Sun⁶, Wenshu Qu⁴, Qing Ye⁷

¹Material Science and Technology Institute, Nanjing University of Aeronautics and Astronautics, Yu-Dao-Str. No. 29, Nanjing, China; ²Post-Doctoral Scientific Research Station in Nanjing General Hospital of Nanjing Military Region, Zhong-Shan-East-Str. No. 305, Nanjing, China; ³Drug Research Institute, Jiangsu Xiansheng Pharmaceutical Company, Xuan-Wu-Str. No. 699, Nanjing, China; ⁴Department of Oncology, The 81 Hospital of The Chinese People's Liberation Army, Tai-Ping-South-Str. No. 147, Nanjing, China; ⁵Department of Oncology, Bengbu Medical College, Dong-Hai-Str. No. 2600, Bengbu, China; ⁶Department of Radiotherapy, Jiangsu Province Hospital, Guang-Jou-Str. No. 300, Nanjing, China; ⁷Department of Pathology, Nanjing Drum Tower Hospital, Zhong-Shan-Str. No. 321, Nanjing, China

Received September 6, 2016; Accepted November 24, 2016; Epub July 15, 2017; Published July 30, 2017

Abstract: The present study aimed to assess the combined effects of Endostar and radiotherapy (RT) in hepatocellular carcinoma (HCC) treatment, and study the pathways involved. Using an HCC transplantation tumor mouse model, we analyzed tumor inhibition rates for as well as the survival of tumor-bearing mice treated by combination therapy. The expression of VEGF, KDR and MVD were analyzed. Cell-based apoptosis and proliferation assays were also used. The combined Endostar and RT group had a mean tumor volume of 8 mg/kg which was less than that in the monotherapy group, and the tumor inhibition rate was 63.59% versus 40% for controls (P<0.05). The combination group had a longer median survival time, 55.6 days, and greater percentage of apoptotic cells than those in the monotherapy group (P<0.05, for both). RT alone increased the expression of VEGF (38.7 \pm 5.8). Combination therapy reduced VEGF (15.0 \pm 1.8), KDR (10.9 \pm 2.9), and MVD (8.6 \pm 1.3) expression compared to controls (P<0.05). Moreover, combination therapy regulated the expression of genes controlling angiogenesis and cell adhesion. Endostar alone inhibited cell proliferation (P<0.05), but the effect on HepG2 cells was weak. Our results demonstrate a synergistic effect of Endostar combined with RT against HCC in vivo and in vitro.

Keywords: Endostar, radiotherapy, HCC, synergistic effects

Introduction

Hepatocellular carcinoma (HCC) is one of the most common malignant tumors in China and typically has with an insidious onset. Because the tumor is well vascularized, it is highly invasive and metastatic. Patients with HCC generally have a poor prognosis as well as a short survival time [1]. Thus, new strategies are needed for the treatment of HCC.

A number of studies have indicated that neovascularization is closely related to the progression and metastasis of tumors [2]. The growth of tumors depends on the nutrients and oxygen transported by the neovascular system. Hence, much research has focused on inhibiting neovascular formation within tumors and consequent starvation of the tumors. This is known as anti-angiogenic therapy. Cancer angiogenesis inhibitors have been widely studied as treatments for hepatoma in both preclinical and clinical research [3-6].

Endostar (recombinant human endostatin) was created by the addition of 9 amino acids to natural endostatin. Endostatin is an endogenous inhibitor of angiogenesis and a 20-kDa C-terminal fragment derived from type XVIII collagen. It is a broad-spectrum angiogenesis inhibitor. Endostar is stable with a longer half-life and higher biological activity than endostatin [7].

Endostar was approved by the State Food and Drug Administration (SFDA) for the treatment of non-small cell lung cancer (NSCLC) in 2005. Phase III and IV clinical studies have verified that combining Endostar with standard chemotherapy regimens improved the median survival time and overall survival of patients with advanced NSCLC [8]. Compared with TC (paclitaxel and carboplatin) alone, TC combined with Endostar treatment reduced the risk of disease progression at an early time point (24 weeks) and increased the objective response rate (ORR). Therefore, it can be used as a first-line treatment for advanced NSCLC. TC combined with Endostar treatment has been found to have good safety and tolerability, improving the quality of life without serious adverse effects or toxicity in patients with advanced NSCLC [9]. Some studies have shown that Endostar is relatively safe and has no significant side effects [10-13].

The effects of Endostar on HCC have been rarely studied. Vessels in non-tumorous liver tissue can be affected by HCC and contribute to tumor growth [14]. For these reasons, targeting tumor vasculature and angiogenesis should be a prominent strategy in anticancer therapy. However, anti-angiogenic agents do not directly kill cancer cells, and this fact is important in considering the use of anti-angiogenic agents.

The application of 3D conformal radiotherapy (3D CRT) has made radiotherapy (RT) one of the main treatments for HCC [15-17], because it can directly kill cancer cells. However, local recurrence and distant metastases are the main causes of RT failure [18]. The key factor that results in the local recurrence of tumors is the presence of tumor cells and vascular endothelial cells that are resistant to radiation [18]. Therefore, decreasing radiation resistance, increasing radiation sensitivity, and inhibiting metastases are of significant clinical relevance.

The combination of an anti-angiogenic agent with RT may be a better treatment for cancer patients [19-21]. Brow et al. have shown that vascular endothelial cells can also develop radio-resistance, which may be one mechanism by which tumors are protected from radiation [22]. Many preclinical studies show that Endostatin can improve the radiotherapeutic effects against many malignant tumors [23,

24]. However, the effect of Endostar combined with RT on HCC remains unclear. In the present study, we aimed to determine whether a synergistic effect exists between Endostar and RT in a subcutaneous transplantation HCC tumor model in mice.

Materials and methods

Determination of the optimum biological dose of Endostar in combination with RT

Imprinting Control Region (ICR) mice aged 5-6 weeks with body weights in the range of 18.0-22.0 g were purchased from Nanjing University Model Animal Research Center (Nanjing, China) and evenly split into groups of males and females. Mice were allowed to acclimate to local conditions for at least 1 week and maintained under a 12-h dark, 12-h light cycle with food and water available ad libitum. The animal use protocol was reviewed and approved by the Institutional Animal Care and Use Committee of Nanjing General Hospital of Nanjing Military Command (Nanjing, China). A murine cancer cell line, H22, was obtained from the Shanghai Institute of Biological Science of the Chinese Academy of Sciences and was passaged. Mouse ascites was used to form tumors in vivo [25]. H22 cells were collected and diluted with saline to a density of 1×10⁷/ml. The tumor cell suspension (0.1 ml) was inoculated into the right hind legs of mice to generate the tumor model. The mice were randomly separated into groups of 10 when the major diameter of the tumors reached 5 mm. Various doses (2, 4, 8, 16, and 32 mg/kg) of Endostar were administered intraperitoneally (i.p.) to the Endostar and combined treatment groups every day for 21 days, whereas saline was used as a control for the remaining groups. The safety of Endostar doses was evaluated in our previous study [25], and no drug-induced hematological toxicity, hepatotoxicity, or liver and kidney injury was observed. RT (10 Gy, once) was administered to the RT groups at day 7 after treatment with Endostar. Electron (6 MeV, 4 Gy/min) beams (Medical linear accelerator, Varian 2100C/D, USA) were used to directly target the tumor with a square radiation field of 3×3 cm. The sourceto-skin distance (SSD) was 100 cm. Major and minor diameters were measured every other day. Tumor volume was calculated as V = $A \times B2 \times \pi/6$ (V = volume, A = major diameter, B =

minor diameter). Mice were sacrificed and necropsied after treatment on the 21st day.

Survival analysis of tumor-bearing mice

After the tumor model was established as described in preceding section, the mice were divided into six groups of 30 mice each. Endostar was administered 24 h after H22 cell inoculation. Treatment with Endostar was maintained for 5 weeks, suspended for 2 weeks. and then resumed until all mice died. RT was given on day 7 of Endostar treatment (same as above). On day 21, the tumor growth inhibition (TGI) rate was calculated as: TGI = (tumor volume of the control group - tumor volume of the treatment group)/tumor volume of the control group ×100%. The synergic effect was considered positive only if the p values between the Endostar-only, combinations of the same Endostar dose with RT, and the RT groups were less than 0.05, and if the TGI of the combination therapy group was greater than 40.00%. Survival was analyzed on day 60 using the following formula: the rate of life extension = (average survival time of the treatment group average survival time of the control group)/ average survival time of the treatment group.

Analysis of metastasis and liver function

The mice had restricted access to food and water the night before periorbital puncture for blood samples on day 21. Plasma ALT (alanine aminotransferase) and AST (aspartate aminotransferase) were measured with kits (Jian Cheng Co., China). Body weight, liver weight (wet), and the liver coefficient (wet/body weight) of the mice were analyzed. The liver and lung tissues of tumor-bearing mice were harvested, fixed in 10% formaldehyde, and embedded in paraffin before slide preparation and staining with hematoxylin-eosin (HE) [26]. The stained tissue sections were analyzed microscopically.

Analysis of tumor MVD and expression of VEGF, KDR, and endostatin

Fresh pieces of tumor tissue without necrotic areas were collected and embedded in paraffin. Immunohistochemistry techniques [27] were used to detect microvascular density (MVD) as well as vascular endothelial growth factor (VEGF), kinase insert domain-containing

receptor (KDR), and endostatin expression with an anti-CD31 antibody (Santa Cruz Biotechnology, USA), an anti-VEGF antibody (Chemicon Co., USA), an anti-KDR antibody (BioSource Co., USA), and an anti-endostatin antibody (Abcam, UK), respectively. The expression of VEGF and KDR was confirmed by Western blotting using the same antibodies, and an anti- β -actin antibody (Santa Cruz Biotechnology, USA) for the use of β -actin as a loading control.

Microarray analysis to identify changes in gene expression in tumor tissue after Endostar treatment

The 36 K mouse genome array (Capital Bio Corp., China), which comprises 35,852 70mer oligo probes, representing approximately 25,000 genes of the mouse genome was used [28]. The tumor tissue samples from tumorbearing mice were harvested on day 21, and total RNA was extracted using a Trizol kit. Arrays were scanned with a LuxScan 10 K-A confocal laser scanner (CapitalBio Corp., Beijing, China), and the obtained images were analyzed with LuxScan3.0 software (CapitalBio Corp., Beijing, China). The normalized signal intensity values were generated by a spatial and intensitydependent (LOWESS) normalization method [11] and were further analyzed if the expression level in one group was more than 2-fold that in another group. The functions of filtered genes were annotated using Molecule Annotation System 2.0 (MAS 2.0) (http://bioinfo.capitalbio.com/mas/).

Analysis of apoptosis in tumor cells

Five randomly chosen tumor samples without necrosis from five different mice in each group were cut into 3-µm thick pieces and rinsed with saline. Cell cycle and apoptosis were analyzed by flow cytometry (FACS Calibur, BD) [29] as well as transmission electronic microscopy (JEM-1200EX, Hitachi Limited) [30].

Cell culture proliferation assay

Human umbilical vein endothelial cells (HUV-ECs) were obtained from Science Cell Corp., and the human HCC cell line, HepG2, was obtained from the Shanghai Institute of Biological Science of the Chinese Academy of

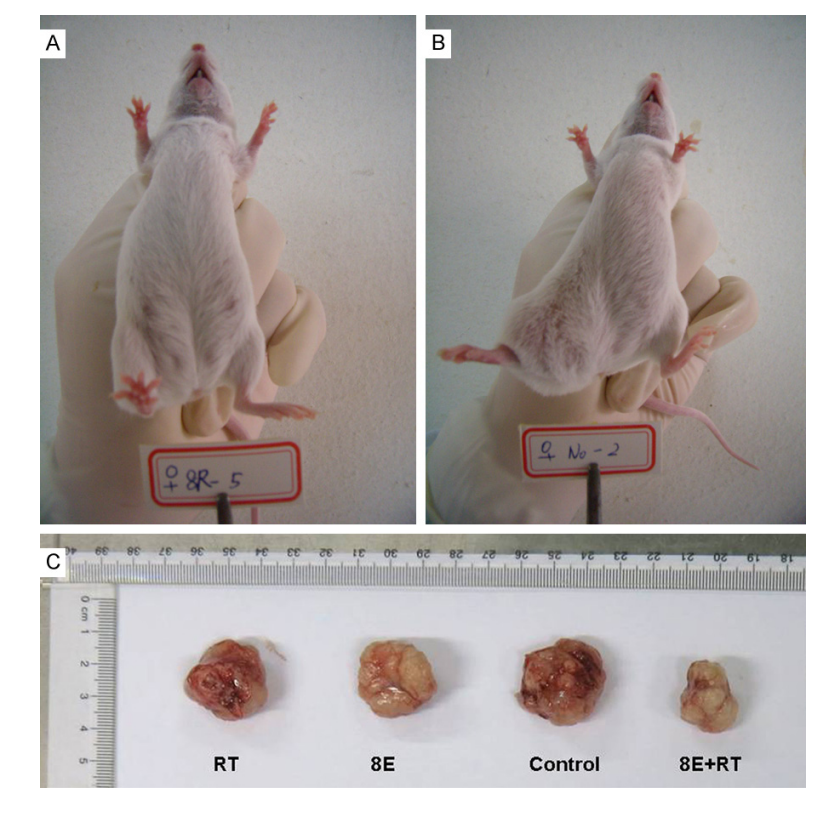


Figure 1. Tumors and the tumor tissues. A. Endostar (4 mg/kg) combined with RT group. B. Negative control group. C. Solid tumor.

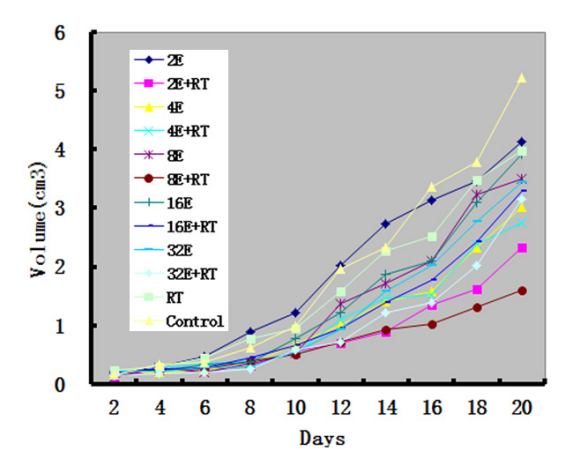


Figure 2. Tumor growth curves.

Sciences. HUVECs and HepG2 cells were maintained in ECM basic medium with 20% fetal bovine serum (FBS) or RPMI 1640 with 10% FBS, respectively, at 37°C in 5% $\rm CO_2$. The cells were plated at a density of $\rm 1\times10^4$ cells/well in 96-well plates, starved for 2 h, and treated with Endostar for 4 h before radiation treatment. Each group had six replicates. Radiation

was administered by a vertical 6-MeV electron beam (Medical linear accelerator, Varian 2100C/D, USA). Cells were maintained in culture for an additional 48 h before an MTT assay to measure proliferation was performed. The cell proliferation rate = (optical density [OD] of the treatment group/OD of the control group) ×100%. These experiments were repeated three times. The synergic effect was considered positive between treatment with Endostar alone, combination of Endostar (same dose) and RT, and RT alone only if the pvalue was less than 0.05, and if the combination therapy group had a lower proliferation rate (actual value) than the additive value (additive value = proliferation rate of Endostar group × proliferation rate of RT group).

Statistical analysis

Statistical Package for Social Sciences (SPSS) software (Version 13.0, SPSS Inc, Chicago, IL, USA) was used for statistical analysis. The results are presented as mean \pm standard deviation (SD) values. Repeated measures, independent non-parametric tests, and one-way analysis of variance were applied for typical data analysis. χ^2 tests were used for rate comparisons, and the Kaplan-Meier analysis was used for survival time analysis. Data were considered statistically significant at P<0.05.

Results

Effects of Endostar doses on inhibition of tumor growth

The treatment groups had smaller tumor volumes than controls. The combined treatment groups, given 4 mg/kg or 8 mg/kg Endostar and RT showed the highest inhibition ability (P<0.05), indicating that the dose-efficacy curve was U-shaped, because higher doses of

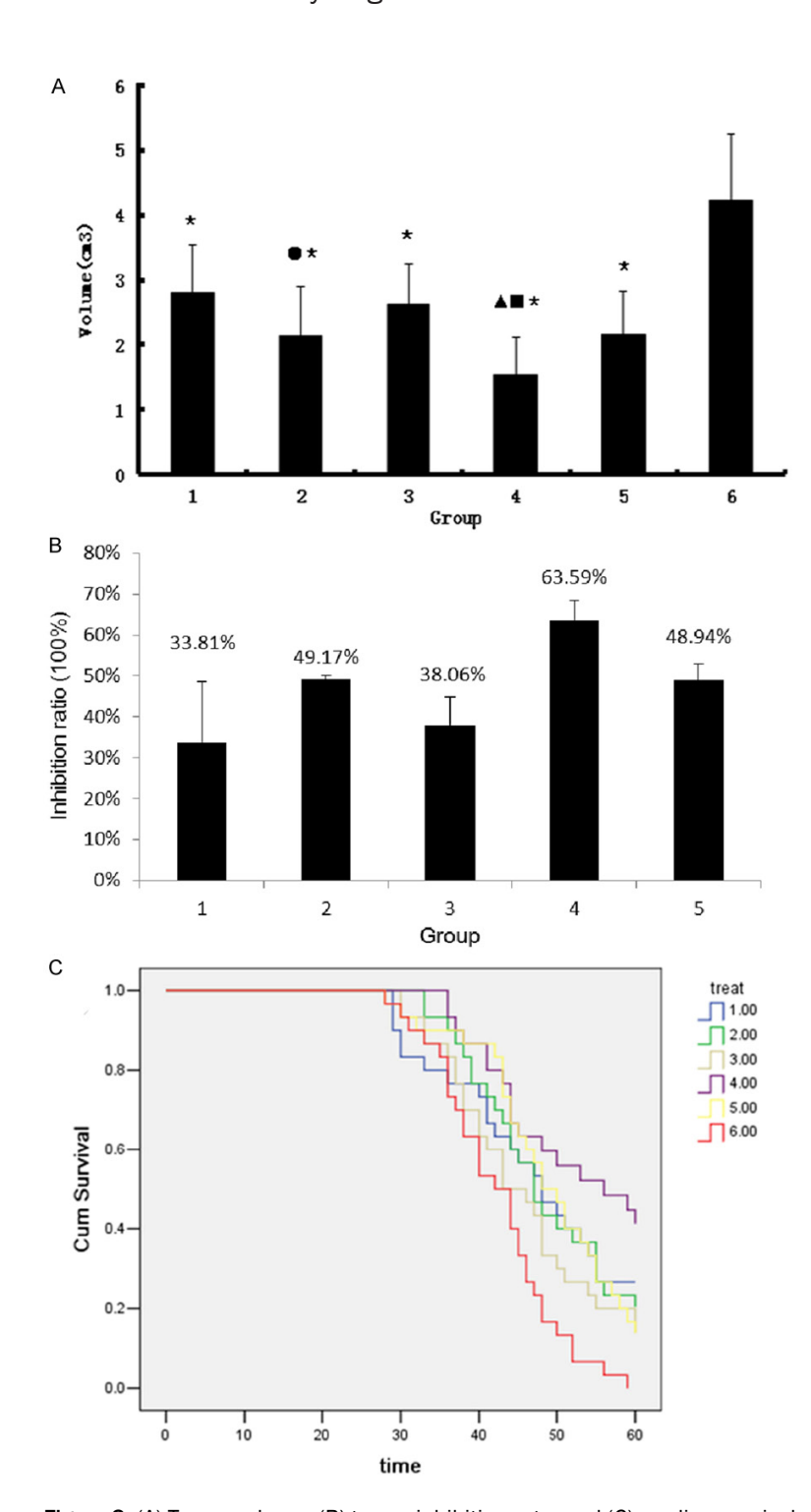


Figure 3. (A) Tumor volume, (B) tumor inhibition rate, and (C) median survival time in the various groups. 1. 4 mg/kg Endostar. 2. 4 mg/kg Endostar combined with RT. 3. 8 mg/kg Endostar. 4. 8 mg/kg Endostar combined with RT. 5. RT only. 6. Control. *P<0.01, compared with group 6; ■P<0.05, compared with group 5; ▲ P<0.05, compared with group 3; ●P<0.01, compared with group 1.

Endostar did not always lead to a higher inhibition effect (Figures 1, 2).

Survival time of tumor-bearing mice after treatment

Based on the optimal biological dose study, 4 mg/kg or 8 mg/kg Endostar was administered alone or in combination with RT to study the effects on the survival of tumorbearing mice. Tumor volumes were measured, and groups that received treatment had significantly smaller tumor volumes than the negative control group (P<0.01). The group treated with 8 mg/kg Endostar combined with RT had a significantly smaller tumor volume than either monotherapy group (P<0.05), with an inhibition rate of 63.59% compared to 40% for controls. The median survival times for the control, RT alone, 8 or 4 mg/kg Endostar plus RT, and 8 mg/kg Endostar alone groups were 43.0, 49.0, 55.6, 46.7, and 45.0 days, respectively. There was a significant difference between these groups (P<0.01). The rate of life extension in the 8 mg/kg Endostar plus RT group was 29.3% (Figure 3).

Metastatic cancer cells in liver

Lungs and livers were harvested after sacrificing the tumor-bearing mice. Five randomly chosen mice from each group were used to make six slides from each tissue, which were stained with HE. In the negative control group, the outline of the central veins of the hepatic lobules was undetectable or blurred, the hepatic cords looked abnormal, and many inflammatory cells had infiltrated the tissue.

Metastatic cancer cells were observed in liver tissue, frequently represented by giant cell

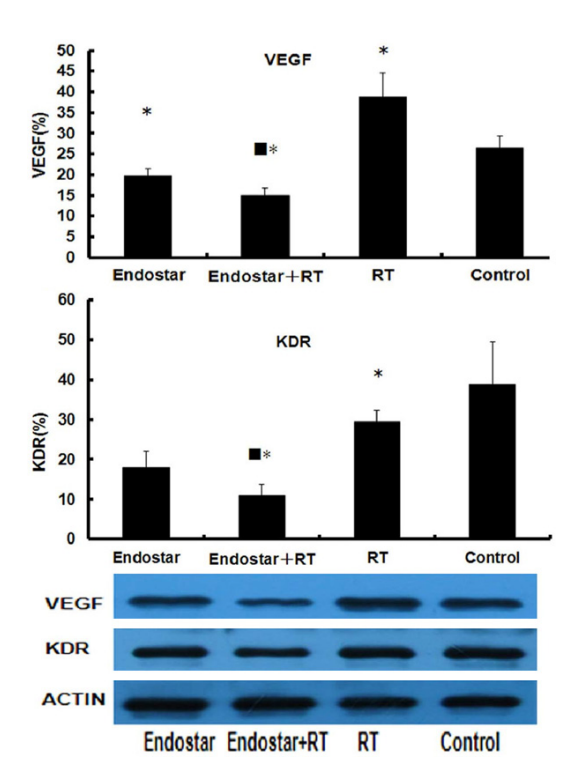


Figure 4. VEGF and KDR protein levels after treatment. *P<0.05, compared with control; ■P<0.05, compared with RT only.

tumors as well as multinucleated cells. The metastasis rate in the negative control group was 66.7%, which was significantly higher than that in the 8 mg/kg Endostar-only group (43.3%) and the RT-only group (53.3%; P<0.05). The 8 mg/kg Endostar plus RT group had the lowest metastasis rate at 26.7% (P<0.05). Lung metastasis was not observed in either group, although an inflammatory response was observed in some lung tissues (Supplemental Data). Liver coefficient, body weight, ALT, and AST did not differ significantly between the Endostar, RT, Endostar+RT (P>0.05; Supplemental Data).

Effects of Endostar combined with RT on MVD and VEGF and KDR expression

A low power lens (100×) was used to find areas with relatively high vascular density as well as high contrast against the tumor background. Then, a high power lens (200×) was used, and four fields were randomly chosen within these areas to calculate the MVD. The results indicated that Endostar combined with RT significantly reduced tumor MVD (P<0.01). Western blotting and immunohistochemistry both indicated that the combination therapy reduced

the expression of VEGF and KDR, although this tumor model had high levels of VEGF and KDR expression in the tumor tissue [31] (P<0.05; Figure 4; Supplemental Data). Compared with the control group, the Endostar group showed significantly greater endostatin deposition (P<0.05; Supplemental Data).

Analysis of microarray data

After three independent comparisons, 123 genes were found to be differentially expressed between the combination therapy group and the RT-only group, including 100 upregulated genes and 23 downregulated genes. The average fold changes in the expression of genes are listed partially in **Table 1**.

Effects of Endostar combined with RT on apoptosis in tumor cells

The flow cytometric data indicated that Endostar combined with RT induced increased levels of apoptosis in tumor cells as well as arrest of the cell cycle at S phase, whereas RT alone caused G2/M arrest. This phenomenon may be due to fact that the specimens were collected on day 14. Tumor cells exposed to both Endostar and RT may have undergone DNA repair and regrowth after treatment, but before collection (Figure 5). There were distinguishing characteristics of tumor cells on electron microscopic examination of the various groups (Supplemental Data).

Differential effects of the combination of Endostar and RT on the proliferation of HUVECs and HepG2 cells

Endostar alone inhibited the proliferation of HUVECs and HepG2 cells, generating a U-shaped dosage curve showing that HUVECs were more sensitive to Endostar than HepG2 cells. Combinations of 0.5 μ g/ml Endostar and 1 or 2 Gy of radiation or 5 μ g/ml Endostar and 0.5, 1, 2, or 4 Gy of radiation had synergic effects, inhibiting HUVEC proliferation. Combinations of 100 μ g/ml Endostar and 1 or 2 Gy of radiation or 200 μ g/ml Endostar and 0.5, 1, 2, or 4 Gy of radiation synergistically inhibited HepG2 proliferation (Tables 2, 3; Figure 6).

Discussion

The liver is a well-vascularized organ. Thus, vascular endothelial cells in HCC are very sensitive

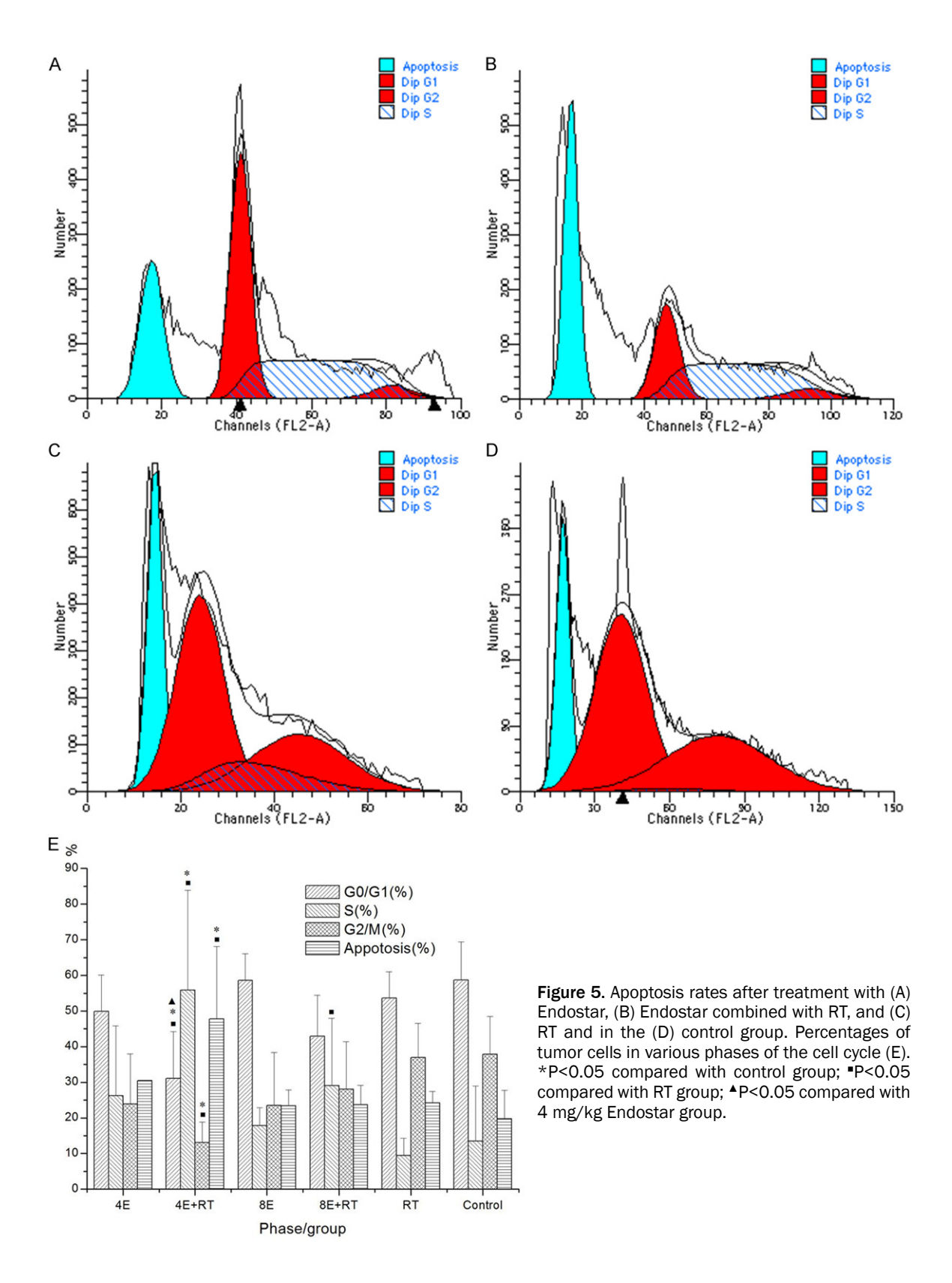
Table 1. Gene expression with radiotherapy alone compared to that with combination therapy

Genebank No.	Gene name	Comments	Ratio
NM_009129	Scg2	Secretogranin II precursor (SgII)	30.9903
NM_009502	VcI	Vinculin	15.5730
NM_011280	Trim10	Tripartite motif protein 10	12.2098
NM_010382	Н2-Еβ1	Histocompatibility 2, class II antigen E beta (H2-Eβ1)	5.2426
NM_207105	H2-Ab1	Response to metastatic cancers 1 (Rmcs1)	4.7480
NM_010378	Η2-Αα	Histocompatibility 2, class II antigen A, alpha (H2-Aα)	4.5842
NM_009144	Sfrp2	Secreted frizzled-related sequence protein 2	3.0919
NM_004401	Dffa	DNA fragmentation factor alpha subunit	0.4472
NM_031161	Cck	Cholecystokinin (Cck)	0.3339
NM_008361	111β	Interleukin 1 beta (II1β)	0.2991

to angiogenic growth factors [4-6]. Targeting tumor vasculature and angiogenesis is thus a prominent strategy in anticancer therapy. Li et al. found that Endostar combined with dexamethasone exhibited synergistic effects on angiogenesis and hepatoma growth [14]. In the current research, the H22 mouse cell line was selected because a review of the literature did not show that endostatin was expressed by H22 cells. In addition, other reports by Li et al. and Xia et al. showed that significant amounts endogenous endostatin were not present in H22 mouse cells [32, 33].

The schedule of combination therapy is critical for achieving a synergic effect when a combination of an anti-angiogenic and RT is used [34, 35]. SU5416 (a VEGFR inhibitor) was administered continuously for 2 weeks before a single dose of radiation (10 or 20 Gy), which resulted in a synergic therapeutic effect [36]. Ansiaux et al. found that the tumor microenvironment began to change after 2 days of thalidomide treatment [37]. This was primarily due to improved oxygenation and blood flow with reduced interstitial pressure in the tumor, which increased the sensitivity of the tumor cells to radiation. Another report [38] also showed that tumor-associated blood vessels are twisted, dilated, and leaky, which leads to poor oxygen and blood flow around tumor tissue. Tumor cells are in a chronic state of high interstitial pressure, oxygen deprivation, and decreased pH, all of which can decrease their sensitivity to radiation. Anti-angiogenic agents may achieve their synergic effect by remodeling immature tumor-associated vessels into functional vessels through inhibition of the VEGF and matrix metalloproteinase (MMP) pathways. There is a window of normalization caused by anti-angiogenics, and administration of RT within this window may be critical to obtaining the maximal therapeutic effect. Williams et al. reported that ZD6474 (a VEGFR2 inhibitor) achieved the synergic effect only when given after RT, not before [39]. This raises a question about the mechanisms of different anti-angiogenic agents, which may result in different ideal treatment schedules when combined with RT. In the current work, RT was given 7 days after treatment with Endostar, with continuous Endostar treatment administered after RT, resulting in a synergic therapeutic effect. We also found that the dose of Endostar used with RT can affect the results.

In terms of tumor volume, Endostar administration in mice that received HCC implants had a U-shaped pattern of dose-effectiveness in our experiments. The U-shaped dose-effectiveness of Endostar was also found in a study by Jiang et al., which showed synergistic effects of Endostar combined with β-elemene in the treatment of malignant ascites in a mouse model [25]. Similar U-shaped responses have been reported for other anti-angiogenic treatments such as angiostatin [40] and interferon-α [41]. However, the mechanism by which U-shaped dose-effectiveness occurs with endostatin is not clear. It is possible that the peptide has multiple targets that have different affinities. High affinity targets, when saturated by ligand may have inhibitory effects through this or other receptors. Other receptors may have low affinity. Once activated, low affinity receptors may become dominant accounting for the increased effects as concentrations are increased.



Studies on tissue distribution and localization of endostatin in animals have been reported

[42-46], and endostatin was shown to be rapidly and widely distributed in the liver, kidneys,

Table 2. Endostar combined with radiotherapy inhibited HUVEC proliferation

OD	0 μg/ml Endostar	0.5 µg/ml Endostar	5 μg/ml Endostar	25 µg/ml Endostar	100 µg/ml Endostar	200 µg/ml Endostar
O Gy	1.07±0.03	0.95±0.08*	0.87±0.10*	1.01±0.10	0.97±0.09	1.05±0.05
0.5 Gy	0.92±0.12	0.80±0.10	0.69±0.05 ^{*,∎,} ▲	0.84±0.09	0.88±0.04	0.87±0.11
1 Gy	0.91±0.08	0.77±0.07*,■,▲	0.66±0.06*,■,▲	0.90±0.05	0.88±0.12	0.93±0.08
2 Gy	0.72±0.06	0.64±0.03*,■,▲	0.49±0.04*,■,▲	0.73±0.04	0.74±0.03	0.72±0.07
4 Gy	0.65±0.06	0.636±0.05	0.44±0.04*,■,▲	0.68±0.14	0.68±0.05	0.59±0.05
6 Gy	0.42±0.04	0.44±0.03	0.46±0.04	0.45±0.06	0.44±0.04	0.37±0.05

Note: *P<0.01 compared with negative control group; *P<0.01 compared with the same dose group of Endostar alone (no radiotherapy); *P<0.01 compared with the same dose group of radiation alone (no Endostar).

Table 3. Endostar combined with radiotherapy inhibited HepG2 cell proliferation

OD	0 μg/ml Endostar	0.5 μg/ml Endostar	5 µg/ml Endostar	25 μg/ml Endostar	100 µg/ml Endostar	200 µg/ml Endostar
O Gy	1.09±0.08	1.15±0.07	1.15±0.04	1.12±0.07	1.06±0.09	0.98±0.09*
0.5 Gy	1.06±0.13	1.03±0.04	1.01±0.11	0.99±0.06	0.95±0.09	0.84±0.03**,■,▲
1 Gy	1.05±0.08	1.06±0.15	1.11±0.08	1.05±0.07	0.92±0.05**,■,▲	0.82±0.05**,■,▲
2 Gy	0.89±0.05	0.93±0.05	0.90±0.08	0.90±0.05	0.80±0.02**,■,▲	0.66±0.04**,■,▲
4 Gy	0.82±0.03	0.83±0.06	0.86±0.05	0.86±0.14	0.77±0.05	0.62±0.04**,■,▲
6 Gy	0.60±0.04	0.62±0.03	0.65±0.05	0.63±0.06	0.62±0.04	0.55±0.05

Note: *P<0.05, **P<0.01 compared with negative control group; *P<0.01 compared with the same dose group of Endostar alone (no radiotherapy); *P<0.01 compared with the same dose group of radiation alone (no Endostar).

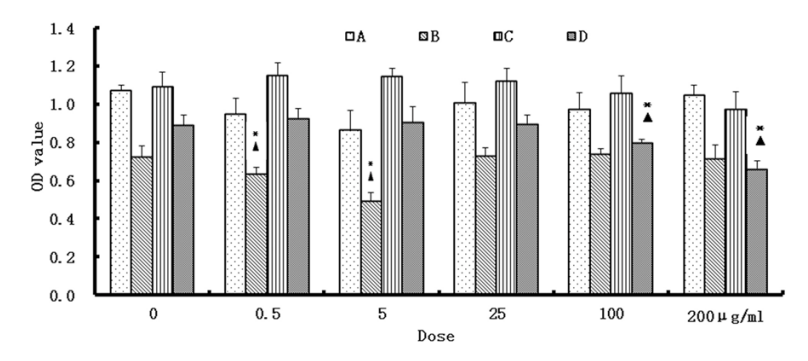


Figure 6. Proliferation of (A) HUVECs exposed to Endostar only, (B) HUVECs exposed to Endostar plus 2 Gy radiation, (C) HepG2 cells exposed to Endostar alone, (D) HepG2 cells exposed to Endostar plus 2 Gy radiation. *P<0.01, compared with the same dose of Endostar alone; ▲ P<0.01, compared with the same dose RT alone.

and tumor tissue. In the current study, we found the Endostar group showed significantly greater endostatin deposition compared with the control group.

Tumor-associated blood vessel endothelial cells are abnormal because they proliferate and renew quickly, dividing every few days [47]. To maintain microcirculation within tumor tissue, endothelial cell stimulation to divide by different growth factors, secreted mainly by tumor

cells, is indispensable, VEGF is one of the most important growth factors driving tumorassociated angiogenesis [48, 49] and was reported to be associated with tumor MVD as well as tumor volume [50]. VEGF can also protect blood vessel endothelial cells from radiation by maintaining the stability of endothelial cells and increasing the motility and invasiveness of tumor cells [51], mediating the resistance of tumors to RT [52]. Shintani et al. reported overexpression of VEGF in tumors

is related to radiation resistance [53]. Several types of tumors show increased VEGF expression after RT, whereas treatment with a VEGF antagonist can sensitize tumors to RT [54-57]. Lee et al. reported that U87 tumors stop growing after RT, but this effect was short-lived, as the tumors grow quickly after the short-term growth inhibition [58]. When treated with a VEGF antibody, tumors became more sensitive to radiation, and the inhibitory growth effect became more stable. This phenomenon was

related to decreased MVD and increased oxygen levels, which could increase the sensitivity of tumors to radiation and antagonize the hypoxia-mediated resistance of tumors to RT. The current experiments also suggest that radiation increased VEGF expression, whereas Endostar decreased it. Endostar inhibits endothelial cell proliferation and decreases VEGF protection of endothelial cells. It might damage vessel endothelial cells synergistically when combined with RT. This may be one of the mechnisms by which Endostar combined with RT inhibited tumor progression.

Moreover, the expression of KDR, which is the most important functional receptor of VEGF, was also downregulated by Endostar and the inhibition of HUVEC proliferation was also observed in vitro. This may explain why the combination has a greater effect than a simple additive effect. MAS analysis was applied to annotate the functions of differentially expressed genes. Most of these genes are involved in angiogenesis, cell adhesion, signal transduction, or apoptosis. Among these genes, Scg2 is involved in cancer angiogenesis; Vcl, Trim10, H2-Eβ1, H2-Ab1, and H2-Aα are involved in cell adhesion; Sfrp2 is involved in Wnt signaling; and Dffa and II1β are apoptosis-related genes. All of the above results suggest that the synergistic effect was achieved not only by reducing tumor MVD, but also by regulating other pathways such as cell adhesion, which is reinforced by the inhibition of metastasis after the combination treatment. Combined treatment with Endostar and RT significantly inhibited liver metastasis, which may be because combination therapy decreased MVD, induced apoptosis of tumor cells, or altered the expression of cell adhesion molecules.

In the current study, RT alone increased VEGF expression, but reduced tumor MVD, which appears contradictory, but can be explained as follows: 1) radiation can damage blood vessel endothelial cells as well as vessel structures; 2) upregulation of VEGF expression by radiation usually takes 1-2 weeks to reach its peak, but the animals were sacrificed 2 weeks after RT, when VEGF upregulation still cannot compensate for the damage of blood vessels by RT; and 3) at a certain time point after RT, tumor cells begin to die, so the amount of growth factors secreted by tumor cells is decreased. As tumor cells that survive radiation reach a hypoxic state, their secretion of growth factors increases to counteract this stress. In the current study, the tumor volume still slowly increased after RT, and VEGF secretion peaked 1-2 weeks after RT. Therefore, MVD, and VEGF and KDR expression were detected at the 2-week time point after RT.

Apoptosis is one of many mechanisms by which tumor and normal cell populations are controlled. Animal survival depends not only on apoptosis [59], but also on tumor proliferation [60], host immune response [61], and location [62], metastases [63], and many other factors. Therefore, it is quite possible to have a dose of therapeutic agent affect only apoptosis and not benefit overall survival.

In conclusion, Endostar together with RT combines the cytotoxicity of radiation and the anti-angiogenic effects of Endostar. These findings provide substantial experimental evidence to support the use of combination therapy against HCC in clinical practice. The present study is a preliminary study on the combination of Endostar with RT for the treatment HCC. The underlying mechanisms and others therapeutic combinations require further study.

Acknowledgements

This paper is supported by "the Fundamental Research Funds for the Central Universities", NO.: NS2014062.

Disclosure of conflict of interest

None.

Address correspondence to: Shukui Qin, Department of Oncology, The 81 Hospital of The Chinese People's Liberation Army, Tai-Ping-South-Str. No. 147, Nanjing 210002, Jiangsu, China. Tel: +86 25 85878181; Fax: +86 25 85878181; E-mail: qinsk00@sina.com

References

- El-Serag HB. Hepatocellular carcinoma. N Engl J Med 2011; 365: 1118-1127.
- [2] Zhou J, Wang L, Xu X, Tu Y, Qin S and Yin Y. Antitumor activity of endostar combined with radiation against human nasopharyngeal carcinoma in mouse xenograft models. Oncol Lett 2012; 4: 976-980.
- [3] Welker MW and Trojan J. Anti-angiogenesis in hepatocellular carcinoma treatment: current evidence and future perspectives. World J Gastroenterol 2011; 17: 3075-3081.

- [4] Raoul J, Santoro A, Beaugrand M, Marrero J, Moscovici M, Shan M, Nadel A, Voliotis D, Bruix J and Llovet J. Efficacy and safety of sorafenib in patients with advanced hepatocellular carcinoma according to ECOG performance status: a subanalysis from the SHARP trial. ASCO Annual Meeting Proceedings 2008; 26: 4587.
- [5] Finn RS and Zhu AX. Targeting angiogenesis in hepatocellular carcinoma: focus on VEGF and bevacizumab. Expert Rev Anticancer Ther 2009; 9: 503-509.
- [6] Ye Q, Qin S, Liu Y, Feng J, Wu Q, Qu W and Yin X. Inhibitory effect of endostar on specific angiogenesis induced by human hepatocellular carcinoma. Gastroenterol Res Pract 2015; 2015: 957574.
- [7] Ling Y, Yang Y, Lu N, You QD, Wang S, Gao Y, Chen Y and Guo QL. Endostar, a novel recombinant human endostatin, exerts antiangiogenic effect via blocking VEGF-induced tyrosine phosphorylation of KDR/Flk-1 of endothelial cells. Biochem Biophys Res Commun 2007; 361: 79-84.
- [8] Sun Y, Wang J, Liu Y, Song X, Zhang Y, Li K, Zhu Y, Zhou Q, You L and Yao C. Results of phase III trial of rh-endostatin (YH-16) in advanced non-small cell lung cancer (NSCLC) patients. ASCO Annual Meeting Proceedings 2005; 23: 7138.
- [9] Han BH, Xiu QY, Wang HM, Shen J, Gu AQ, Luo Y, Bai CX, Guo SL, Liu WC, Zhuang ZX, Zhang Y, Zhao YZ, Jiang LY, Shi CL, Jin B, Zhou JY and Jin XQ. [A multicenter, randomized, double-blind, placebo-controlled safety study to evaluate the clinical effects and quality of life of paclitaxel-carboplatin (PC) alone or combined with endostar for advanced non-small cell lung cancer (NSCLC)]. Zhonghua Zhong Liu Za Zhi 2011; 33: 854-859.
- [10] Huang R, Zhan Q, Zhou X, Chu Z, Jiang J and Liang X. Continuous administration of recombinant human endostatin (endostar): a preclinical safety study. Exp Ther Med 2012; 3: 1018-1022.
- [11] Li Y, Huang XE, Yan PW, Jiang Y and Xiang J. Efficacy and safety of endostar combined with chemotherapy in patients with advanced solid tumors. Asian Pac J Cancer Prev 2010; 11: 1119-1123.
- [12] Wang J, Li K, Sun T, Zhang MJ, Li WL, Yao Q, Liu W, Ding CM, He ZY, Mao WD, Wang HM, Zhang Y and Zhou XL. [Efficacy and safety of rh-end-ostatin combined with docetaxel in second-line or intolerant toxicity for first-line treatment in patients with advanced non-small cell lung cancer]. Zhonghua Zhong Liu Za Zhi 2013; 35: 618-622.
- [13] Zhang LP, Liao XY, Xu YM, Yan LJ, Yan GF, Wang XX, Duan YZ and Sun JG. Efficacy and safety of endostar(R) combined with chemotherapy in patients with advanced soft tissue sarcomas.

- Asian Pac J Cancer Prev 2013; 14: 4255-4259.
- [14] Li XQ, Shang BY, Wang DC, Zhang SH, Wu SY and Zhen YS. Endostar, a modified recombinant human endostatin, exhibits synergistic effects with dexamethasone on angiogenesis and hepatoma growth. Cancer Lett 2011; 301: 212-220.
- [15] Yoon HI and Seong J. Optimal selection of radiotherapy as part of a multimodal approach for hepatocellular carcinoma. Liver Cancer 2016; 5: 139-151.
- [16] Komatsu S, Hori Y, Fukumoto T, Murakami M, Hishikawa Y and Ku Y. Surgical spacer placement and proton radiotherapy for unresectable hepatocellular carcinoma. World J Gastroenterol 2010; 16: 1800-1803.
- [17] Gomes AR, Abrantes AM, Brito AF, Laranjo M, Casalta-Lopes JE, Goncalves AC, Sarmento-Ribeiro AB, Botelho MF and Tralhao JG. Influence of P53 on the radiotherapy response of hepatocellular carcinoma. Clin Mol Hepatol 2015; 21: 257-267.
- [18] Peng F, Xu Z, Wang J, Chen Y, Li Q, Zuo Y, Chen J, Hu X, Zhou Q, Wang Y, Ma H, Bao Y and Chen M. Recombinant human endostatin normalizes tumor vasculature and enhances radiation response in xenografted human nasopharyngeal carcinoma models. PLoS One 2012; 7: e34646.
- [19] Mazeron R, Anderson B, Supiot S, Paris F and Deutsch E. Current state of knowledge regarding the use of antiangiogenic agents with radiation therapy. Cancer Treat Rev 2011; 37: 476-486.
- [20] Morganti AG, Cellini F, Mignogna S, Padula GD, Caravatta L, Deodato F, Picardi V, Macchia G, Cilla S, Buwenge M, Di Lullo L, Gambacorta MA, Balducci M, Mattiucci GC, Autorino R and Valentini V. Low-dose radiotherapy and concurrent FOLFIRI-bevacizumab: a phase II study. Future Oncol 2016; 12: 779-787.
- [21] Firtina Karagonlar Z, Koc D, Iscan E, Erdal E and Atabey N. Elevated hepatocyte growth factor expression as an autocrine c-Met activation mechanism in acquired resistance to sorafenib in hepatocellular carcinoma cells. Cancer Sci 2016; 107: 407-416.
- [22] Brown CK, Khodarev NN, Yu J, Moo-Young T, Labay E, Darga TE, Posner MC, Weichselbaum RR and Mauceri HJ. Glioblastoma cells block radiation-induced programmed cell death of endothelial cells. FEBS Lett 2004; 565: 167-170.
- [23] Ling CH, Ji C, Chen YB, Fu JX, Zhou JY, Chen WC, Yang JC and Su LY. [Combined effects of endostatin gene transfer and ionizing radiation on lung adenocarcinoma model of A549-cells]. Zhonghua Jie He He Hu Xi Za Zhi 2004; 27: 683-686.

- [24] Luo X, Andres ML, Timiryasova TM, Fodor I, Slater JM and Gridley DS. Radiation-enhanced endostatin gene expression and effects of combination treatment. Technol Cancer Res Treat 2005: 4: 193-202.
- [25] Jiang ZY, Qin SK, Yin XJ, Chen YL and Zhu L. Synergistic effects of endostar combined with beta-elemene on malignant ascites in a mouse model. Exp Ther Med 2012; 4: 277-284.
- [26] Becker M, Ingianni G, Lassner F, Atkins D and Schroder JM. [Intraoperative histological sections in obstetric brachial plexus lesions-comparison of macroscopic appearance, HE staining and toluidine blue staining]. Handchir Mikrochir Plast Chir 2003; 35: 112-116.
- [27] Huang C, Huang R, Chang W, Jiang T, Huang K, Cao J, Sun X and Qiu Z. The expression and clinical significance of pSTAT3, VEGF and VEGF-C in pancreatic adenocarcinoma. Neoplasma 2012; 59: 52-61.
- [28] Yan X, Chen H, Lu X, Wang F, Xu W, Jin H and Zhu P. Fascaplysin exert anti-tumor effects through apoptotic and anti-angiogenesis pathways in sarcoma mice model. Eur J Pharm Sci 2011; 43: 251-259.
- [29] Chu QD, Sun G, Pope M, Luraguiz N, Curiel DT, Kim R, Li BD and Mathis JM. Virotherapy using a novel chimeric oncolytic adenovirus prolongs survival in a human pancreatic cancer xenograft model. Surgery 2012; 152: 441-448.
- [30] Jung Y, Nam SW and Agarwal R. High-resolution transmission electron microscopy study of electrically-driven reversible phase change in ge2sb2te5 nanowires. Nano Lett 2011; 11: 1364-1368.
- [31] Zheng QP CL, Shi YS. Effect of radiation combined with anti-VEGF monoclonal antibody on angiogenic factors in human hepatocellular carcinoma xenografts. Chinese Journal of Cancer Prevention and Treatment 2008; 15: 1852-1855.
- [32] Li PY, Lin JS, Feng ZH, He YF, Zhou HJ, Ma X, Cai XK and Tian DA. Combined gene therapy of endostatin and interleukin 12 with polyvinylpyrrolidone induces a potent antitumor effect on hepatoma. World J Gastroenterol 2004; 10: 2195-2200.
- [33] Qi X, Liu Y, Wei W, Huang X and Zuo Y. Effects of the C-terminal of endostatin on the tumorigenic potential of H22 cells. Biomed Rep 2013; 1: 761-765.
- [34] Huang SM, Li J, Armstrong EA and Harari PM. Modulation of radiation response and tumorinduced angiogenesis after epidermal growth factor receptor inhibition by ZD1839 (Iressa). Cancer Res 2002; 62: 4300-4306.

- [35] Winkler F, Kozin SV, Tong RT, Chae SS, Booth MF, Garkavtsev I, Xu L, Hicklin DJ, Fukumura D and di Tomaso E. Kinetics of vascular normalization by VEGFR2 blockade governs brain tumor response to radiation: role of oxygenation, angiopoietin-1, and matrix metalloproteinases. Cancer Cell 2004; 6: 553-563.
- [36] Schuuring J, Bussink J, Bernsen HJ, Peeters W and van Der Kogel AJ. Irradiation combined with SU5416: microvascular changes and growth delay in a human xenograft glioblastoma tumor line. Int J Radiat Oncol Biol Phys 2005; 61: 529-534.
- [37] Ansiaux R, Baudelet C, Jordan BF, Beghein N, Sonveaux P, De Wever J, Martinive P, Grégoire V, Feron O and Gallez B. Thalidomide radiosensitizes tumors through early changes in the tumor microenvironment. Clin Cancer Res 2005; 11: 743-750.
- [38] Jain RK. Normalization of tumor vasculature: an emerging concept in antiangiogenic therapy. Science 2005; 307: 58-62.
- [39] Williams KJ, Telfer BA, Brave S, Kendrew J, Whittaker L, Stratford IJ and Wedge SR. ZD6474, a potent inhibitor of vascular endothelial growth factor signaling, combined with radiotherapy: schedule-dependent enhancement of antitumor activity. Clin Cancer Res 2004; 10: 8587-8593.
- [40] Lalani AS, Chang B, Lin J, Case SS, Luan B, Wu-Prior WW, VanRoey M and Jooss K. Anti-tumor efficacy of human angiostatin using livermediated adeno-associated virus gene therapy. Mol Ther 2004; 9: 56-66.
- [41] Slaton JW, Perrotte P, Inoue K, Dinney CP and Fidler IJ. Interferon-alpha-mediated down-regulation of angiogenesis-related genes and therapy of bladder cancer are dependent on optimization of biological dose and schedule. Clin Cancer Res 1999; 5: 2726-2734.
- [42] Yang XX, Hu ZP, Chan E, Duan W and Zhou S. Pharmacokinetics of recombinant human endostatin in rats. Curr Drug Metab 2006; 7: 565-576.
- [43] He GA, Xue G, Xiao L, Wu JX, Xu BL, Huang JL, Liang ZH, Xiao X, Huang BJ, Liu RY and Huang W. Dynamic distribution and expression in vivo of human endostatin gene delivered by adenoviral vector. Life Sci 2005; 77: 1331-1340.
- [44] Herbst RS, Hess KR, Tran HT, Tseng JE, Mullani NA, Charnsangavej C, Madden T, Davis DW, McConkey DJ, O'Reilly MS, Ellis LM, Pluda J, Hong WK and Abbruzzese JL. Phase I study of recombinant human endostatin in patients with advanced solid tumors. J Clin Oncol 2002; 20: 3792-3803.
- [45] Yang DJ, Kim KD, Schechter NR, Yu DF, Wu P, Azhdarinia A, Roach JS, Kalimi SK, Ozaki K, Fogler WE, Bryant JL, Herbst R, Abbruzzes J, Kim

- EE and Podoloff DA. Assessment of antiangiogenic effect using 99mTc-EC-endostatin. Cancer Biother Radiopharm 2002; 17: 233-245.
- [46] Strik HM, Schluesener HJ, Seid K, Meyermann R and Deininger MH. Localization of endostatin in rat and human gliomas. Cancer 2001; 91: 1013-1019.
- [47] Li M, Ye C, Feng C, Riedel F, Liu X, Zeng Q and Grandis JR. Enhanced antiangiogenic therapy of squamous cell carcinoma by combined endostatin and epidermal growth factor receptorantisense therapy. Clin Cancer Res 2002; 8: 3570-3578.
- [48] Pinheiro C, Garcia EA, Morais-Santos F, Moreira MA, Almeida FM, Jube LF, Queiroz GS, Paula EC, Andreoli MA, Villa LL, Longatto-Filho A and Baltazar F. Reprogramming energy metabolism and inducing angiogenesis: co-expression of monocarboxylate transporters with VEGF family members in cervical adenocarcinomas. BMC Cancer 2015; 15: 835.
- [49] Chen H, Shen YF, Gong F, Yang GH, Jiang YQ and Zhang R. Expression of VEGF and its effect on cell proliferation in patients with chronic myeloid leukemia. Eur Rev Med Pharmacol Sci 2015; 19: 3569-3573.
- [50] Szubert S, Moszynski R, Michalak S, Nowicki M, Sajdak S and Szpurek D. The associations between serum VEGF, bFGF and endoglin levels with microvessel density and expression of proangiogenic factors in malignant and benign ovarian tumors. Microvasc Res 2016; 107: 91-96.
- [51] Kaliski A, Lassau N, Maggiorella L, Mathe D, Frascogna V, Rouffiac V, Opolon P, Haie-Meder C, Bourhis J and Deutsch E. Antiangiogenic effect and tumor growth control achieved by an MMP-inhibitor combined to radiation in vivo, targeting radio-induced MMP-2 enhancement and VEGF modulation. International Journal of Radiation Oncology* Biology* Physics 2004; 60: S368-S369.
- [52] Gupta VK, Jaskowiak NT, Beckett MA, Mauceri HJ, Grunstein J, Johnson RS, Calvin DA, Nodzenski E, Pejovic M, Kufe DW, Posner MC and Weichselbaum RR. Vascular endothelial growth factor enhances endothelial cell survival and tumor radioresistance. Cancer J 2002; 8: 47-54.
- [53] Shintani S, Kiyota A, Mihara M, Nakahara Y, Terakado N, Ueyama Y and Matsumura T. Association of preoperative radiation effect with tumor angiogenesis and vascular endothelial growth factor in oral squamous cell carcinoma. Jpn J Cancer Res 2000; 91: 1051-1057.
- [54] Bischof M, Abdollahi A, Gong P, Stoffregen C, Lipson KE, Debus JU, Weber KJ and Huber PE. Triple combination of irradiation, chemotherapy (pemetrexed), and VEGFR inhibition (SU5416) in human endothelial and tumor cells. Int J Radiat Oncol Biol Phys 2004; 60: 1220-1232.

- [55] Geng L, Donnelly E, McMahon G, Lin PC, Sierra-Rivera E, Oshinka H and Hallahan DE. Inhibition of vascular endothelial growth factor receptor signaling leads to reversal of tumor resistance to radiotherapy. Cancer Res 2001; 61: 2413-2419.
- [56] Park JS, Qiao L, Su ZZ, Hinman D, Willoughby K, McKinstry R, Yacoub A, Duigou GJ, Young CS, Grant S, Hagan MP, Ellis E, Fisher PB and Dent P. Ionizing radiation modulates vascular endothelial growth factor (VEGF) expression through multiple mitogen activated protein kinase dependent pathways. Oncogene 2001; 20: 3266-3280.
- [57] Kermani P, Leclerc G, Martel R and Fareh J. Effect of ionizing radiation on thymidine uptake, differentiation, and VEGFR2 receptor expression in endothelial cells: the role of VEGF (165). Int J Radiat Oncol Biol Phys 2001; 50: 213-220.
- [58] Lee CG, Heijn M, di Tomaso E, Griffon-Etienne G, Ancukiewicz M, Koike C, Park KR, Ferrara N, Jain RK, Suit HD and Boucher Y. Anti-Vascular endothelial growth factor treatment augments tumor radiation response under normoxic or hypoxic conditions. Cancer Res 2000; 60: 5565-5570.
- [59] Kawauchi S, Goto Y, Ihara K, Furuya T, Oga A, Tsuneyoshi M, Kawai S and Sasaki K. Survival analysis with p27 expression and apoptosis appears to estimate the prognosis of patients with synovial sarcoma more accurately. Cancer 2002; 94: 2712-2718.
- [60] Gudlaugsson E, Skaland I, Janssen EA, van Diest PJ, Voorhorst FJ, Kjellevold K, zur Hausen A and Baak JP. Prospective multicenter comparison of proliferation and other prognostic factors in lymph node negative lobular invasive breast cancer. Breast Cancer Res Treat 2010; 121: 35-40.
- [61] Vieira T, Antoine M, Hamard C, Fallet V, Duruisseaux M, Rabbe N, Rodenas A, Cadranel J and Wislez M. Sarcomatoid lung carcinomas show high levels of programmed death ligand-1 (PD-L1) and strong immune-cell infiltration by TCD3 cells and macrophages. Lung Cancer 2016; 98: 51-58.
- [62] Pallud J, Roux A and Zanello M. Relationship between tumour location and preoperative seizure incidence depends on glioma grade of malignancy. Epileptic Disord 2016; 18: 107-108
- [63] Kaseda K, Watanabe K, Asakura K, Kazama A and Ozawa Y. Identification of false-negative and false-positive diagnoses of lymph node metastases in non-small cell lung cancer patients staged by integrated (18F-)fluorodeoxyglucose-positron emission tomography/computed tomography: a retrospective cohort study. Thorac Cancer 2016; 7: 473-480.

Table S1. Proliferation rate of HUVECs with various treatments

Radiation dose		O Gy	0.5 Gy	1 Gy	2 Gy	4 Gy	6 Gy
0 μg/ml Endostar		0.0%	85.5%	84.7%	67.6%	60.9%	39.0%
0.5 µg/ml Endostar	Actual value	88.6%	75.0%	71.8%	59.5%	59.4%	41.3%
0.5 µg/ml Endostar	Additive value	0.0%	75.8%	75.0%	59.9%	54.0%	34.6%
5 μg/ml Endostar	Actual value	80.8%	64.7%	61.9%	46.0%	40.8%	42.6%
5 μg/ml Endostar	Additive value	0.0%	69.1%	68.4%	54.6%	49.2%	31.5%

The actual value of combinations of 0.5 μ g/ml Endostar and 1 or 2 Gy of radiation were 71.8%, 59.5% lower than the additive value (75.0%, 59.9%), moreover the OD value were different between treatment with Endostar 0.5 μ g/ml alone, Endostar (0.5 μ g/ml) combined with 1 or 2 Gy radiation, and the same dose of radioation alone (P<0.05). The actual value of combinations of 5 μ g/ml Endostar and 0.5, 1, 2, or 4 Gy of radiation were 64.7%, 61.9%, 46.0%, 40.8% lower than the additive value (69.1%, 68.4%, 54.6%, 49.2%), moreover the OD value were different between treatment with Endostar 5 μ g/ml alone, Endostar (5 μ g/ml) combined with 0.5, 1, 2, or 4 Gy ray, and the same dose of radiation alone (P<0.05). The combinations of 0.5 μ g/ml Endostar and 1 or 2 Gy of radiation or 5 μ g/ml Endostar and 0.5, 1, 2, or 4 Gy of radiation had synergic effects, inhibiting HUVEC proliferation.

Table S2. Proliferation rate of HepG2 cells with various treatments

Radiation dose		O Gy	0.5 Gy	1 Gy	2 Gy	4 Gy	6 Gy
0 μg/ml Endostar		0.0%	97.4%	96.1%	81.6%	74.9%	54.6%
100 µg/ml Endostar	Actual value	97.0%	87.0%	84.3%	73.2%	70.5%	57.0%
100 µg/ml Endostar	Additive value	0.0%	94.5%	93.2%	79.2%	72.7%	53.0%
200 µg/ml Endostar	Actual value	89.4	77.1%	75.4%	60.8%	56.6%	50.5%
200 μg/ml Endostar	Additive value	0.0%	87.1%	85.9%	73.0%	66.96%	45.1%

The actual value of combinations of 100 μ g/ml Endostar and 1 or 2 Gy of radiation were 84.3%, 73.2% lower than the additive value (93.2%, 79.2%), moreover the OD value were different between treatment with Endostar 100 μ g/ml alone, Endostar (100 μ g/ml) combined with 1 or 2 Gy ray, and the same dose ray alone (P<0.05). The actual value of combinations of 200 μ g/ml Endostar and 0.5, 1, 2, or 4 Gy of radiation were 77.1%, 75.4%, 60.8%, 56.6% lower than the additive value (87.1%, 85.9%, 73.0%, 66.96%). Moreover the OD value were different between treatment with Endostar 200 μ g/ml alone, Endostar (200 μ g/ml) combined with 0.5, 1, 2, or 4 Gy ray, and the same dose of radiation alone (P<0.05). The combinations of 100 μ g/ml Endostar and 1 or 2 Gy of radiation or 200 μ g/ml Endostar and 0.5, 1, 2, or 4 Gy of radiation synergistically inhibited HepG2 proliferation.

Table S3. The ALT, AST, body weight and liver coefficient in various groups

Group	ALT (U/L)	AST (U/L)	Body weight (g)	Liver coefficient (%)
Endostar	297.31±68.26	380.80±54.93	37.99±4.31	3.03±0.47
RT	300.75±66.35	390.39±58.53	37.30±3.72	3.14±0.43
Endostar+RT	295.21±51.71	379.09±59.14	37.64±3.95	3.04±0.41
Control	302.60±59.24	386.82±61.04	38.51±4.03	3.02±0.39

Compared with the control group the liver coefficient, body weight, plasma ALT and AST did not show significant changes (P>0.05) in the Endostar, RT, Endostar+RT group.

Table S4. Optical density of Endostatin staining in various groups

Group	Endostar	Endostar+RT	RT	Control
Endostatin	29905.46±6746.49*	23402.77±7551.43	16261.55±881.49	16782.15±2412.78

^{*}P<0.05, compared with control. Compared with the control group the expression of endostatin in Endostar group showed significant differences (P<0.05).

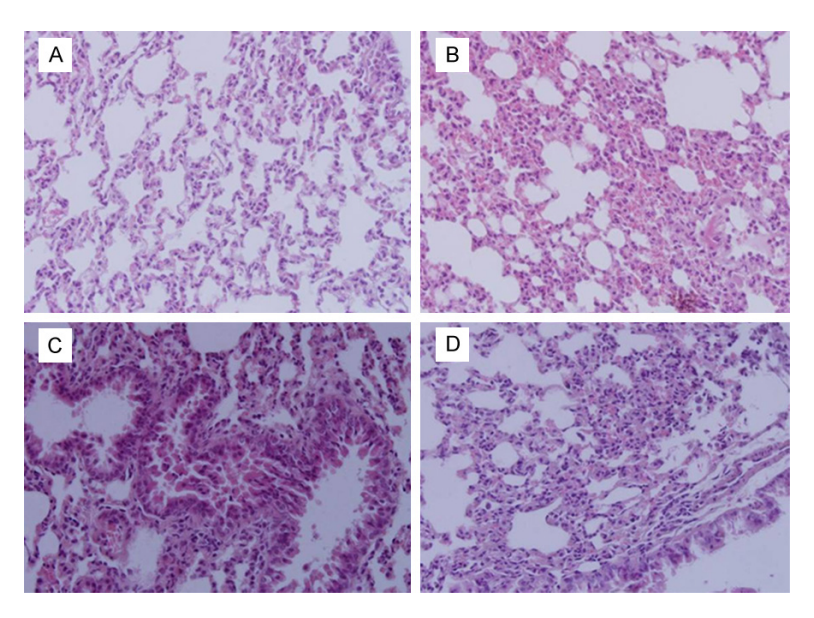


Figure S1. Lung metastasis was not observed in combination or monotherapy groups. There were obvious inflammatory responses in the RT group and the control group, including the following: the alveolar septum became thick, the squamous intraepithelial metaplasia of the bronchiole emerged, and fibrosis was identifiable in alveolar septum. There was atelectasis in the RT group and the control group. The inflammatory response was less in the Endostar-treated animals than in the other groups. A. Representative lung tissue of the Endostar group. B. Representative lung tissue of the Endostar combined with RT group. C. Representative lung tissue of the RT group. D. Representative lung tissue of the control group (100×).

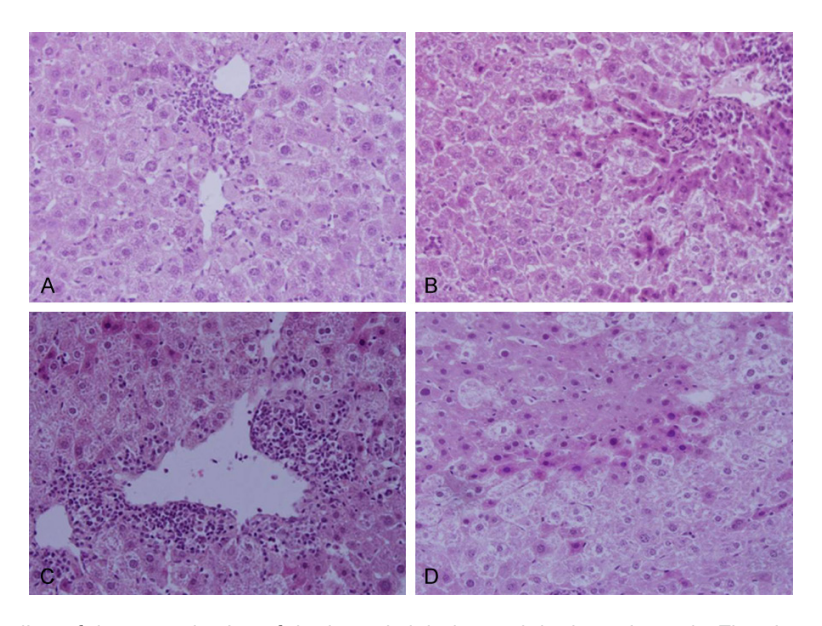


Figure S2. The outline of the central veins of the hepatic lobules and the hepatic cords. The giant-cell tumors, multinucleate cells, and a necrotic zone of hepatocytes could frequently be observed in the control group. The zones of hepatocyte necrosis were close to blood vessels in the RT group, but the pieces of necrotic zone could be identified with difficulty in the Endostar group. We also found smaller zones of hepatocyte necrosis close to blood vessels in

the Endostar combined with RT group compared to the RT-only group. A. Liver tissue of the Endostar group. B. Liver tissue of the Endostar combined with RT group. C. Liver tissue of the RT group. D. Liver tissue of the control group (100×).

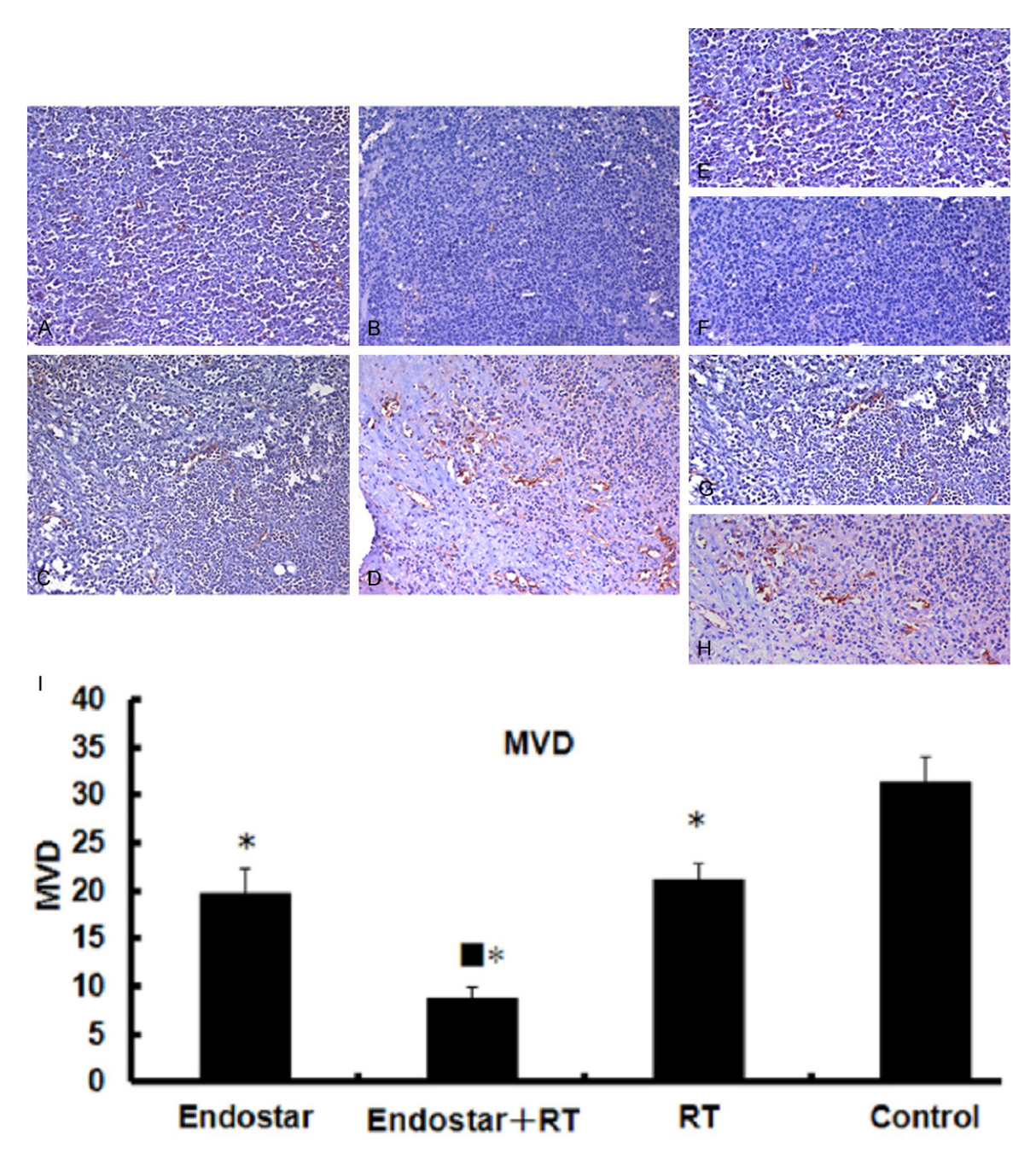


Figure S3. The MVD of tumor tissues. (A) Endostar group (magnification, 100×), (B) Endostar combined with RT group (magnification, 100×), (C) RT-only group (magnification, 100×), (D) control group (magnification, 100×), (E) Endostar group (magnification, 200×), (F) Endostar combined with RT group (magnification, 200×), (G) RT-only group (magnification, 200×), and (H) control group (magnification, 200×), and (I) graph of MVD.

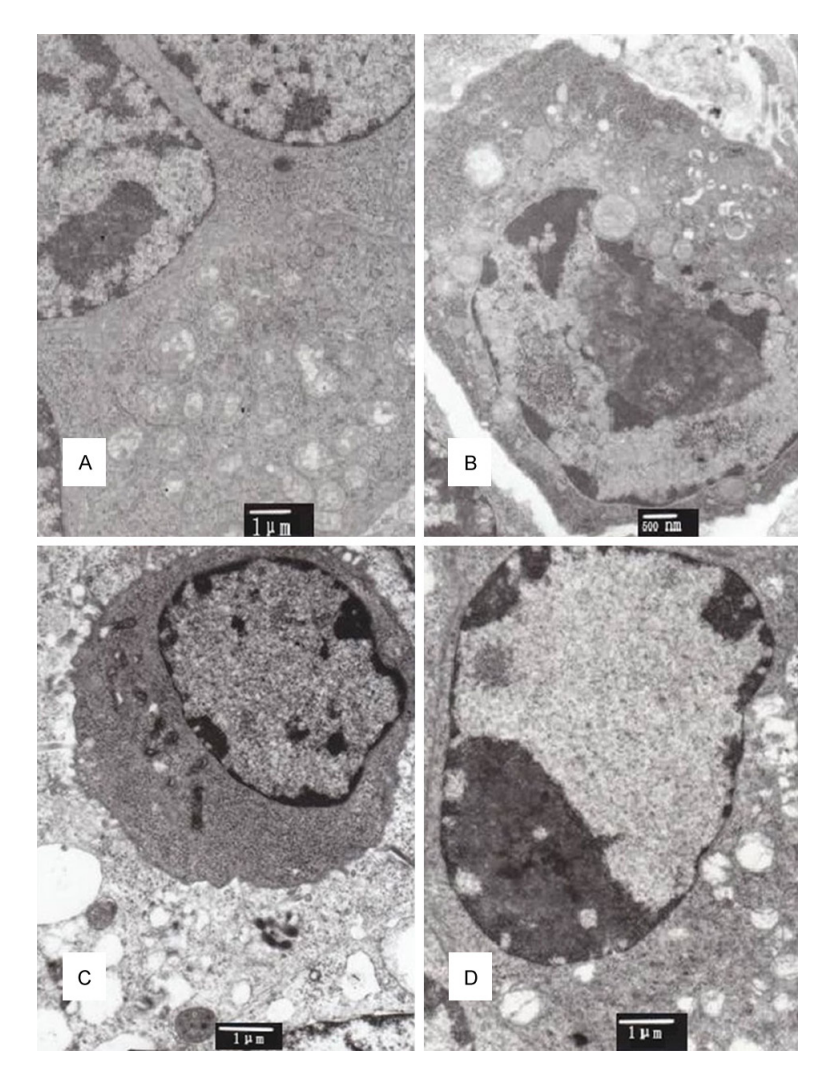


Figure S4. Electron micrographs. A. Mitochondria were obviously swollen, with broken cristae (Endostar group). B. Cell-cell junctions were less apparent, the tumor cells were less dense, and the cytoplasmic organelles were obviously decreased in number in the combined treatment group (Endostar combined with RT). C. Apoptotic cells (RT group). D. Control group. The tumor cell volume was different and nucleoli were grossly enlarged under electron microscopy. In the Endostar-only group, the nucleoli of the tumor cells were obvious. The mitochondria were swollen, and the cristae were broken. The rough endoplasmic reticulum (RER) was abundant, and mild ectasia was present. Glycogen was abundant and uniformly distributed. Apoptotic cells were occasionally identified. In the Endostar combined with RT group, the nucleoli could be identified. The cell-cell junctions were less apparent and the tumor cells were less dense. The organelles in the cytoplasm were obviously decreased in number. The mitochondria were swollen, and the cristae were broken. Glycogen was less abundant than in the Endostar-only group. The apoptotic cells and necrotic cells could be easily identified and were abundant in the combined therapy group. In the RT-only group, the nucleoli and nuclear inclusions could be seen. There were bundles of phlegmonous cells in the matrix. The mitochondria were swollen with broken cristae, and vacuolization was also observed. Apoptotic cells were present. In the control group, the nucleoli and nuclear inclusions could be seen. The mitochondria were somewhat swollen with partially broken cristae. The RER showed mild ectasia. Occasionally, phlegmonous cells in the matrix were identified. There were very few apoptotic cells in the tumor.

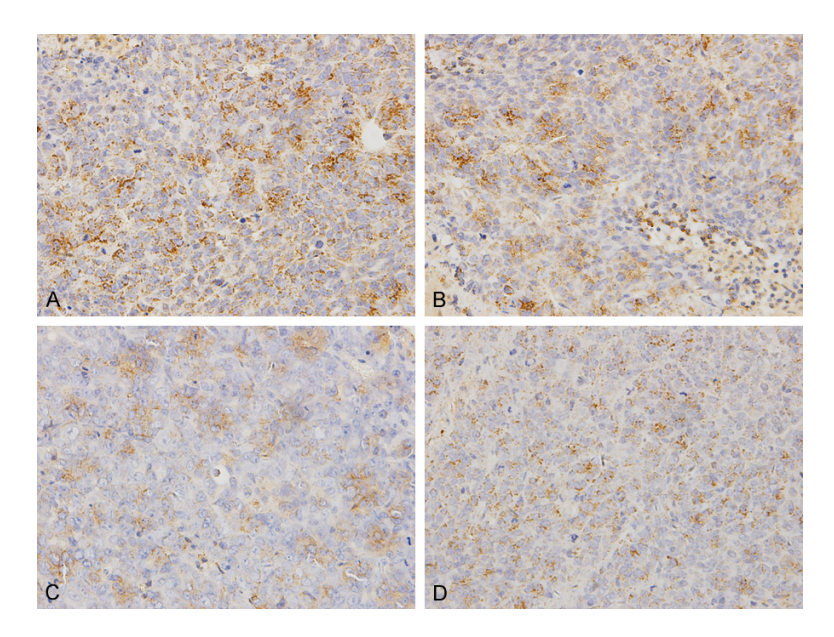


Figure S5. Immunohistochemistry for expression of endostatin after treatment with (A) Endostar, (B) Endostar combined with RT, and (C) RT and in the (D) control group ($100\times$). Compared with the control group, the Endostar mice showed significant differences (P<0.05) in endostatin deposition.